Supplementary Material

Supplementary Material

Contents:

SM1: ^{1}H and ^{13}C NMR spectra
SM2: COSY and HSQC spectra unambiguously establishing the assignment of ^{1}H and ^{13}C NMR signals.
SM3: Comparison of ^{1}H NMR experimental data (left) with spectra simulated using the values in Table II (right)
SM4: 60 Mz simulation of H2–H5 signals using values in Table II (left) compared with experimental spectrum reproduced from Ref. 19 (right)
SM5. The singly occupied molecular orbital of the $1^{2}A^{/}$ state, which is much more compact than the ground state, with higher bow and stern angles.
SM6. The transition state for thermal interconversion of CHT to NCD.
SM7. The HOMO for the transition state for thermal interconversion of CHT to NCD.
SM8. MP3 and MP4SDQ harmonic vibrational frequencies for CHT compared with anharmonic values at the MP2 level, including rotational constants for the vibrationally excited states, some of which are present in the microwave spectrum.
SM9. The singly occupied molecular orbital of the $1^{2}A^{/}$ state, which is much more compact than the ground state, with higher bow and stern angles.
SM10. MP4SDQ harmonic vibrational frequencies for $1^{2}A^{/}$ state of CHT.
SM11. The $X^{2}A^{//}$ surface as a function of the two dihedral angles chosen. See main Paper.
SM12. A 2-dimensional representation of SM11, showing the regular pattern generated as the G-16 'scan' process occurs. See main text for details.
SM13. The avoided crossing under C_1 symmetry of the $^{2}A^{/}$ and $^{2}A^{//}$ states in C_S symmetry.

SM1: ^{1}H and ^{13}C NMR spectra

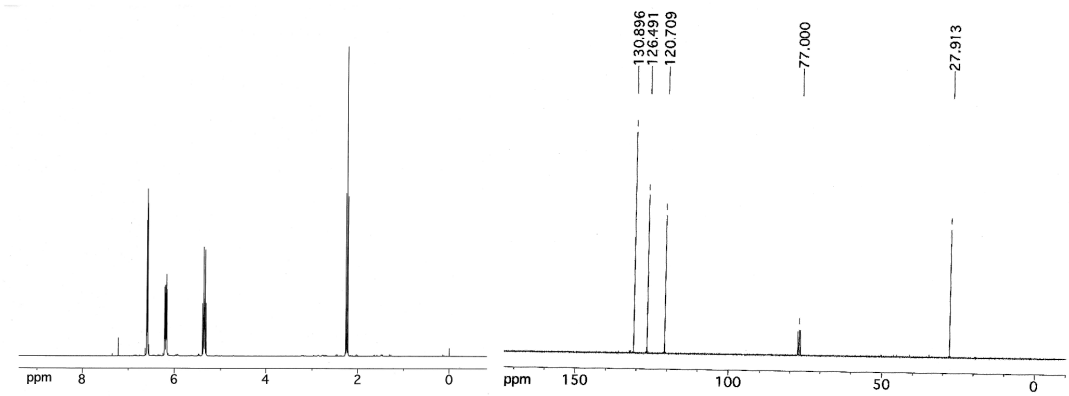

SM2: COSY and HSQC spectra unambiguously establishing the assignment of ^{1}H and ^{13}C NMR signals.

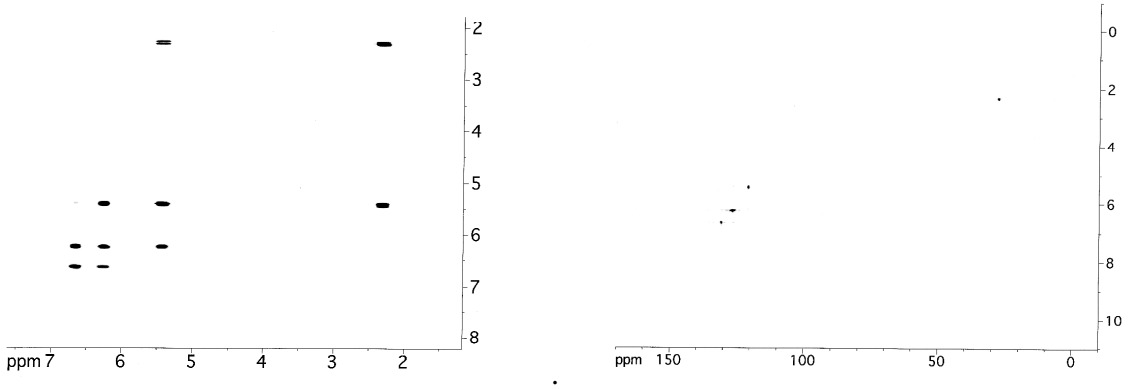

SM3: Comparison of ^{1}H NMR experimental data (left) with spectra simulated using the values in Table II (right)

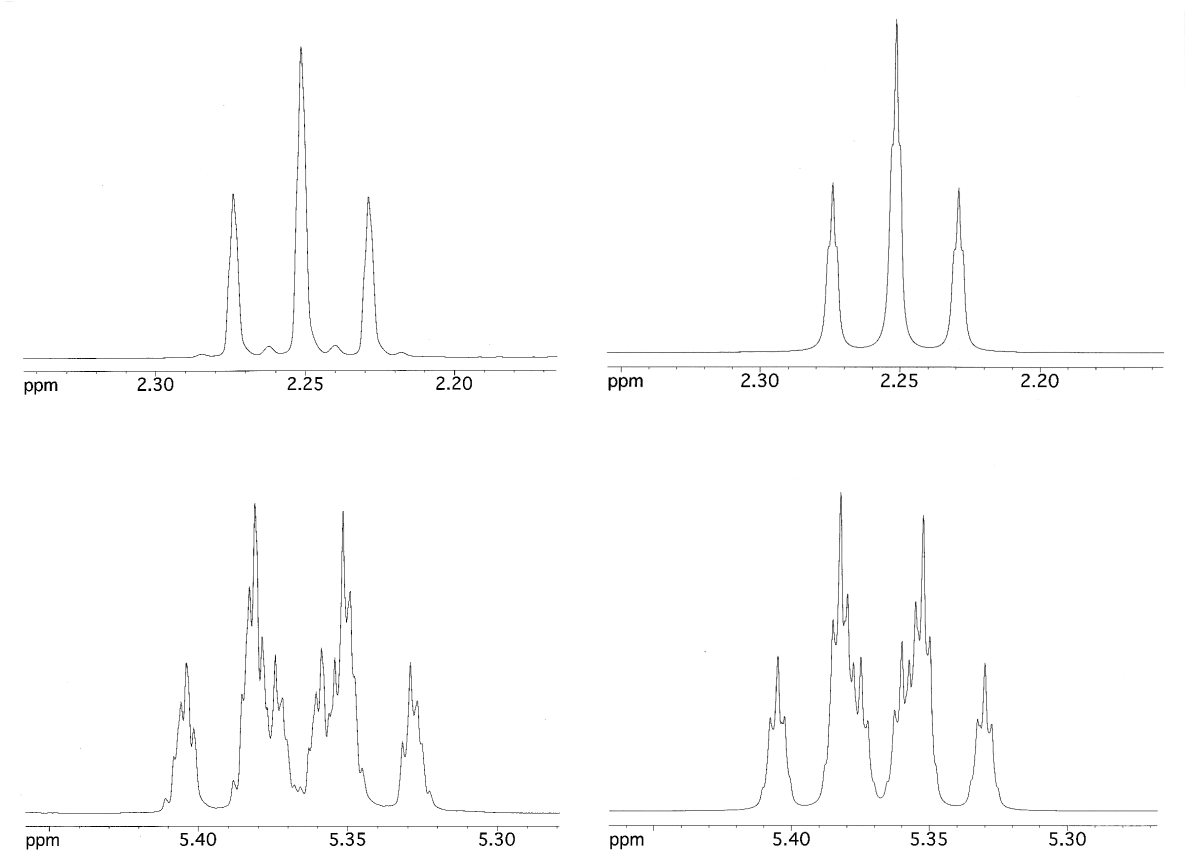

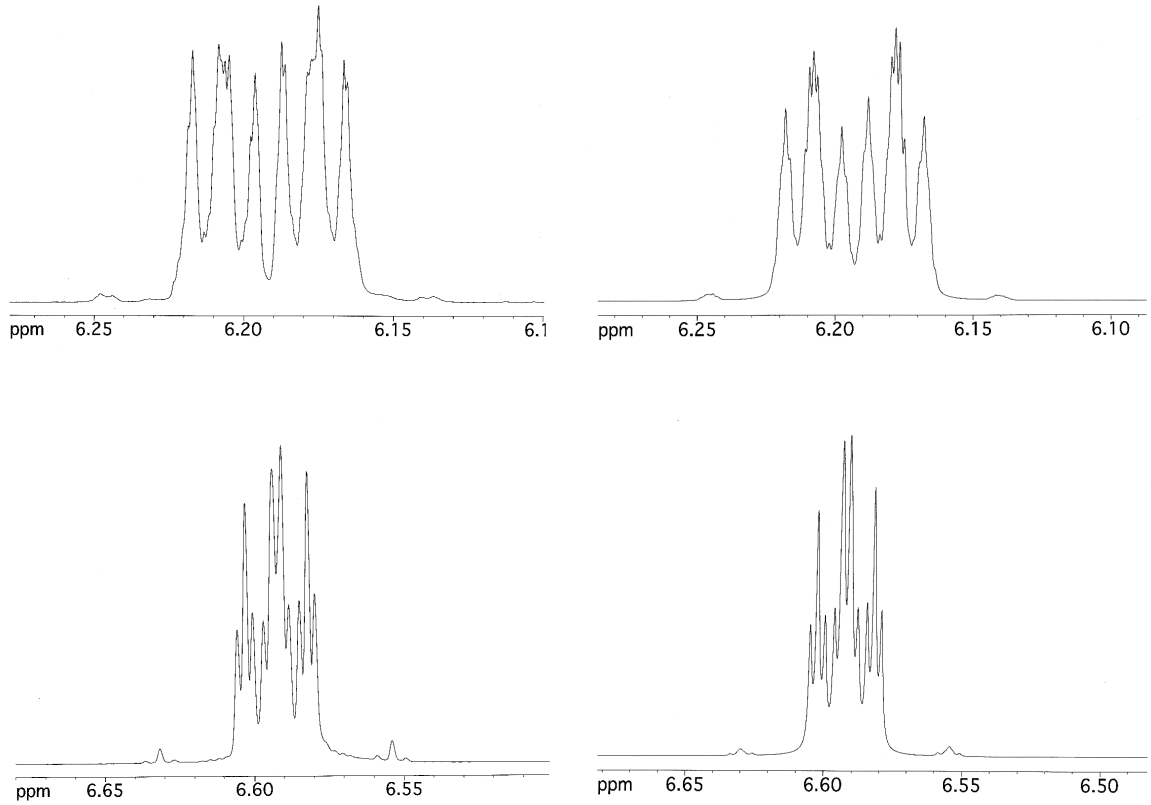

SM4: 60 Mz simulation of H2–H5 signals using values in Table II (left) compared with experimental spectrum reproduced from Ref. 19 (right)

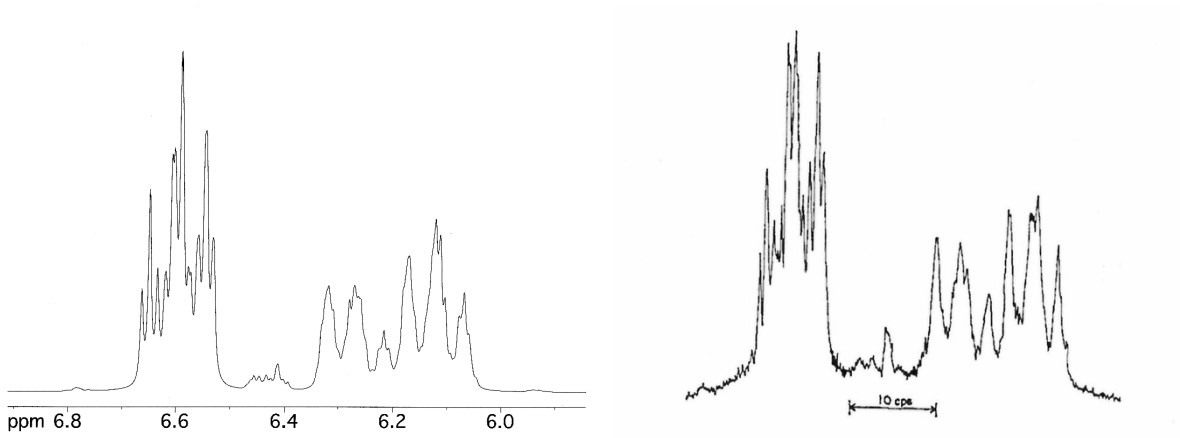

SM5. The singly occupied molecular orbital of the $1^2A'$ state, which is much more compact than the ground state, with higher bow and stern angles.

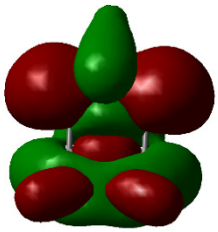

SM6. The transition state for thermal interconversion of CHT to NCD.

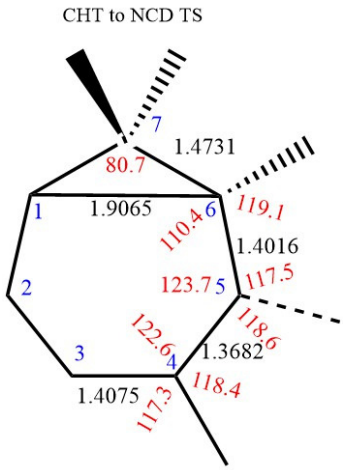

D2165 0.0, D3216 20.0,
D7123 34.3, D2345 0.0

SM7. The HOMO for the transition state for thermal interconversion of CHT to NCD.

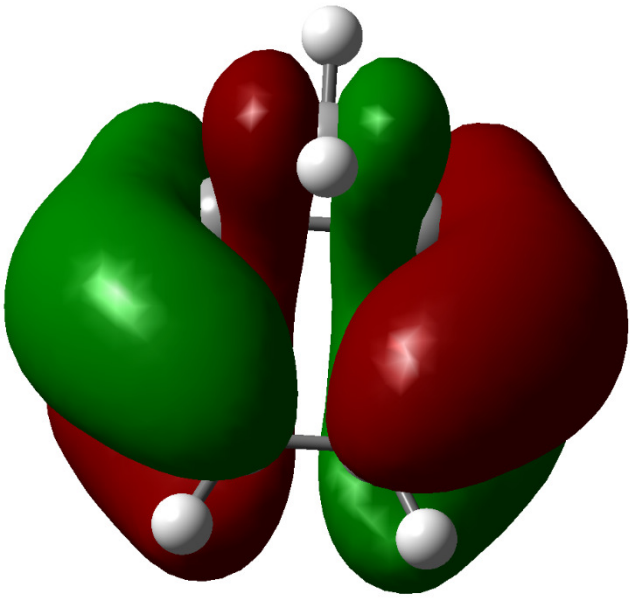

SM8. MP3 and MP4SDQ harmonic vibrational frequencies for neutral CHT compared with anharmonic values at the MP2 level, including rotational constants for the vibrationally excited states, some of which are present in the microwave spectrum.

	MP3	MP4SDQ	MP2 values[a]				
Mode	Harmonic /cm^{-1}	Harmonic /cm^{-1}	Harmonic /cm^{-1}	Anharmonic /cm^{-1}	A / cm^{-1}	B /cm^{-1}	C /cm^{-1}
1	3225.4	3200.8	3208.4	3070.3	3691.9	3673.7	2051.9
2	3213.2	3188.1	3195.8	3036.1	3691.0	3675.2	2052.1
3	3195.6	3171.6	3181.0	3089.1	3692.1	3673.8	2051.9
4	3149.4	3125.0	3152.3	3013.3	3690.4	3676.0	2051.8
5	3058.6	3039.1	3047.3	2940.1	3690.0	3677.4	2051.8
6	1713.7	1701.8	1642.5	1599.0	3692.0	3672.1	2052.4
7	1645.6	1646.0	1556.0	1509.5	3690.4	3671.2	2051.7
8	1514.2	1511.1	1497.9	1455.1	3697.2	3674.9	2053.3
9	1445.7	1440.3	1425.6	1393.6	3691.7	3677.0	2052.4
10	1257.8	1252.7	1239.9	1219.0	3697.6	3674.8	2054.1
11	1235.3	1230.8	1215.2	1191.3	3691.3	3679.3	2053.2
12	1062.1	1057.3	1063.7	1037.4	3685.4	3676.8	2048.7
13	982.7	978.9	968.0	953.5	3687.5	3680.6	2051.2
14	949.4	943.8	947.8	932.5	3686.0	3669.4	2050.1
15	939.4	934.7	933.2	908.3	3690.3	3671.4	2051.8
16	815.4	810.7	810.3	798.7	3689.2	3675.2	2052.9
17	741.8	739.7	722.6	703.1	3693.5	3674.1	2053.8
18	674.4	671.1	664.2	650.7	3695.3	3675.3	2052.2
19	442.7	440.8	424.5	411.9	3693.6	3675.4	2054.3
20	361.4	359.2	347.7	340.7	3698.6	3675.3	2049.2

21	232.4	226.8	256.6	249.1	3692.4	3667.4	2048.5
22	3221.2	3196.7	3204.9	3071.2	3692.1	3673.4	2051.9
23	3200.0	3175.2	3184.6	3052.8	3691.9	3673.9	2051.9
24	3187.1	3162.3	3170.9	3012.8	3691.2	3675.2	2052.1
25	1713.1	1702.2	1648.6	1602.0	3690.7	3670.6	2051.5
26	1496.8	1489.3	1485.0	1450.4	3692.4	3673.3	2051.2
27	1406.0	1401.5	1380.8	1350.2	3693.5	3676.3	2052.8
28	1360.4	1358.3	1325.8	1286.9	3690.4	3673.4	2054.0
29	1294.5	1288.7	1287.3	1250.8	3695.1	3674.3	2052.8
30	1221.9	1218.0	1199.3	1177.5	3693.6	3679.6	2054.4
31	1080.6	1076.6	1084.2	1063.4	3693.5	3674.8	2053.7
32	995.0	992.5	984.5	960.5	3698.4	3669.0	2051.4
33	982.1	977.5	962.9	964.2	3690.6	3672.2	2052.5
34	980.4	976.3	945.8	937.8	3692.7	3673.5	2053.3
35	892.5	888.7	883.5	873.7	3694.6	3675.2	2052.3
36	765.2	761.8	757.5	748.7	3692.8	3673.8	2053.3
37	601.1	597.4	607.0	597.9	3688.8	3674.4	2052.5
38	409.2	406.0	408.5	404.1	3695.3	3676.5	2055.7
39	288.6	287.2	288.5	285.6	3690.4	3677.3	2054.4

Footnote to Table SM8
a Using the conversion factor $h/8\pi^2 = 505\ 531$ MHz.amu.ang^2

The unscaled anharmonic frequencies, shown in Table SM2, are compared with the harmonic series using MP2, MP3 or MP4SDQ. Using the MP4SDQ set for comparison, the MP2 and MP3 harmonic frequencies have correlations close to linear. However, individual modes have

differences up to 90, 59 and -53 cm^{-1}, for modes 6, 7 and 25 respectively. Comparison of the MP2 anharmonic frequencies with the MP4SDQ harmonic set yields a correlation $\nu_{MP2\ anharm} = 0.952(2)\ \nu_{MP4SDQ} + 26(4)\ cm^{-1}$ over all 39 vibrations. If the 8 C-H stretching frequencies are omitted, then the correlation becomes $\nu_{MP2\ anharm} = 0.971(3)\ \nu_{MP4SDQ} + 8(3)\ cm^{-1}$ with correlation coefficient 0.9997, and a mean difference 21 cm^{-1}. Thus, if the C-H stretching modes are excluded, the MP2 anharmonic values are a close comparison with the more rigorous MP4SDQ harmonic values, which we cannot determine at the anharmonic level.

SM9. The singly occupied molecular orbital of the $1^2A'$ state, which is much more compact than the ground state, with higher bow and stern angles.

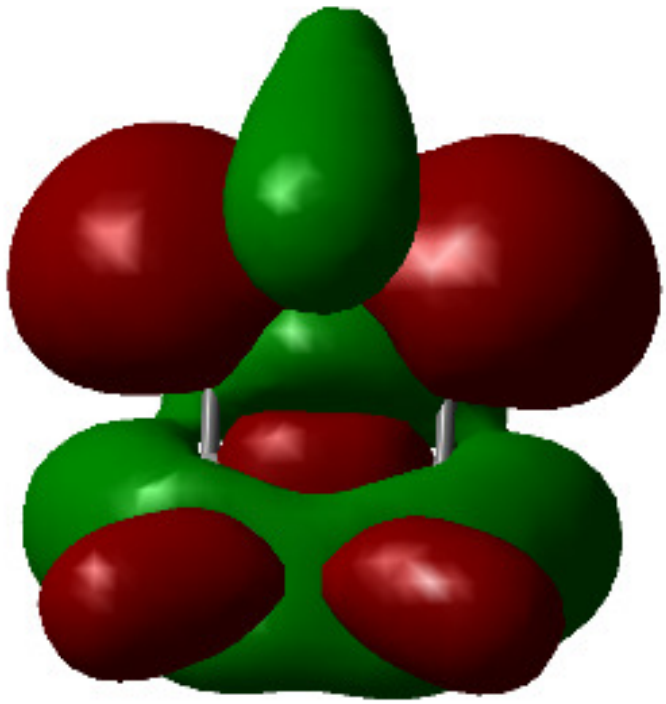

SM10. MP4SDQ harmonic vibrational frequencies for $1^2A'$ state of CHT.

A'	87.6	A'	1265.4
A"	221.9	A"	1300.3
A'	367.5	A'	1318.2

A'	403.9	A"	1440.9
A"	419.1	A'	1441.8
A"	483.4	A"	1457.1
A'	643.1	A'	1495.1
A"	783.0	A"	1527.3
A'	792.0	A"	1571.8
A'	830.0	A'	1607.6
A"	876.4	A'	1671.4
A'	932.5	A'	2940.3
A"	942.7	A'	3140.7
A'	959.2	A"	3211.5
A'	976.9	A'	3217.2
A"	1008.5	A"	3218.9
A"	1035.7	A'	3227.1
A'	1091.8	A"	3238.9
A"	1152.1	A'	3240.2
A"	1245.3		

SM11. The $X^2A^{//}$ surface as a function of the two dihedral angles chosen. See main Paper.

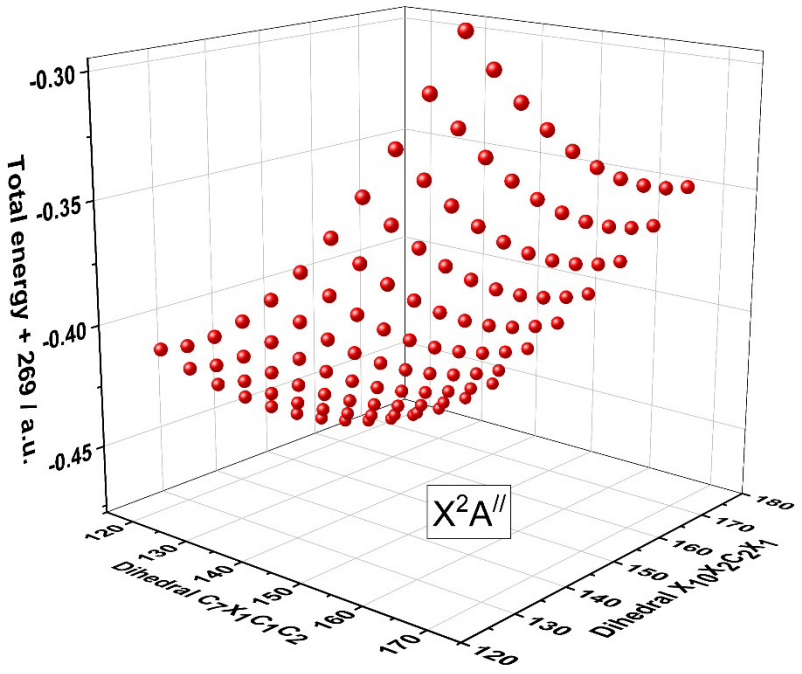

SM12. A 2-dimensional representation of SM13, showing the regular pattern generated as the G-16 'scan' process occurs. See main text for details.

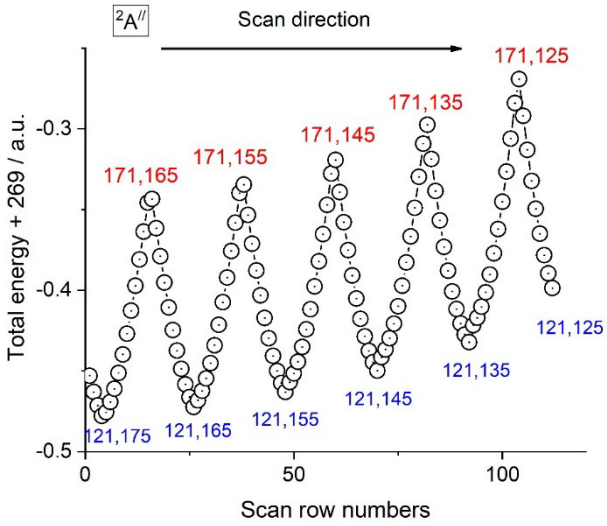

SM13. The avoided crossing under C_1 symmetry of the $^2A'$ and $^2A''$ states in C_S symmetry. The energies fitted have been adjusted by addition of 269.0 a.u.